

# Optimizing Gradient-driven Criteria in Network Sparsity: Gradient is All You Need

Yuxin Zhang<sup>1</sup> Mingbao Lin<sup>1,2</sup> Mengzhao Chen<sup>1</sup> Zihan Xu<sup>1,2</sup> Fei Chao<sup>1</sup> Yunhang Shen<sup>2</sup> Ke Li<sup>2</sup>  
Yongjian Wu<sup>2</sup> Rongrong Ji<sup>1,3</sup>

## Abstract

Network sparsity receives popularity mostly due to its capability to reduce the network complexity. Extensive studies excavate gradient-driven sparsity. Typically, these methods are constructed upon premise of weight independence, which however, is contrary to the fact that weights are mutually influenced. Thus, their performance remains to be improved. In this paper, we propose to further optimize gradient-driven sparsity (OptG) by solving this independence paradox. Our motive comes from the recent advances on supermask training which shows that sparse subnetworks can be located in a randomly initialized network by simply updating mask values without modifying any weight. We prove that supermask training is to accumulate the weight gradients and can partly solve the independence paradox. Consequently, OptG integrates supermask training into gradient-driven sparsity, and a specialized mask optimizer is designed to solve the independence paradox. Experiments show that OptG can well surpass many existing state-of-the-art competitors. Our code is available at <https://github.com/zyxxmu/OptG>.

## 1. Introduction

The explosive advances of convolution neural networks (CNNs) are mainly driven by continuously growing model parameters, incurring deployment difficulty on resource-constrained devices. By directly removing parameters for a sparse model, network sparsity emerges as an important technique to reduce model complexity (LeCun et al., 1989; Mozer & Smolensky, 1989; Hoeffler et al., 2021).

<sup>1</sup>Media Analytics and Computing Laboratory, Department of Artificial Intelligence, School of Informatics, Xiamen University, Xiamen, China <sup>2</sup>Tencent Youtu Lab, Shanghai, China <sup>3</sup>Institute of Artificial Intelligence, Xiamen University, Xiamen, China. Correspondence to: Rongrong Ji <rrji@xmu.edu.cn>.

Broadly speaking, methods in the literature can be divided into after-training sparsity, before-training sparsity and during-training sparsity (Liu et al., 2021a). After-training sparsity aims to remove parameters in pre-trained models (Han et al., 2015), while before-training sparsity attempts to refrain from the time-consuming pre-training process by constructing sparse models at random initialization (Lee et al., 2019). Recent advances advocate during-training sparsity which consults the sparsity process throughout network training (Evci et al., 2020; Kusunuri et al., 2020).

Particularly, the core of network sparsity lies in selecting to-be-removed parameters such that it can satisfy: 1) desired sparse rate; 2) acceptable performance compromise. To this end, the most straightforward solution is to remove these parameters causing least increase on the training loss  $\mathcal{L}$ . Then, by leveraging the first-order Taylor expansion of the loss function  $\mathcal{L}$  to approximate the influence of removing parameter  $\mathbf{w}_i$ , the key format for measuring weight importance can be expressed as  $\frac{\partial \mathcal{L}}{\partial \mathbf{w}_i} \mathbf{w}_i$ , leading to gradient-driven sparsity. Recent advances rewrite this format using higher-order Taylor expansion (Wang et al., 2020; Molchanov et al., 2017), which will be detailed in Sec. 3.1.

Despite the progress, existing gradient-driven methods are built upon premise of independence among weights. However, this assumption contradicts with the practical implementation, in which, parameters are collectively making effort to derive the network output. Usually, existing methods remove weights once-for-all (Lee et al., 2019; Wang et al., 2020). Consequently, the computed loss change used to remove weights deviates a lot from the actual loss change. Thus, it is necessary to overcome this independence paradox in order to pursue a better performance.

Beyond the gradient-driven sparsity, recent developments on supermask training (Zhou et al., 2019; Ramanujan et al., 2020) show that high-performing sparse subnetwork can be located upon a randomly initialized networks without modifying any weight. Instead, they choose to update mask values using the straight-through-estimator (STE) (Bengio et al., 2013). In Sec. 3.3, we innovatively prove that the essence of supermask training is to accumulate gradients of both preserved and removed weights in gradient-driven spar-

sity. Also, we show that this manner can partially solve the independence paradox. Unfortunately, the fixed weights in supermask training fail to eliminate independence paradox, thus, the performance is still sub-optimal.

In this paper, we propose to optimize the gradient-driven sparsity by integrating the advantage of supermask training in overcoming the independence paradox. Our method, termed OptG, introduces a novel mask optimizer that continuously accumulates the mask gradients of each training iteration. Differently, we only update the mask using SGD in the beginning of each training epoch. In this way, the remaining parameters can be well tuned on the training set to minimize the error gap, thus the independence paradox can be well solved. Extensive experiments demonstrate that OptG dominates its counterparts especially in the extreme sparse rate. For instance, OptG removes 98% parameters of ResNet-50 while still achieves 67.20% top-1 accuracy on ImageNet, surpassing the recent strong baseline STR (He et al., 2018) that only reaches 62.84% by a large margin.

Our main contributions are summarized below:

- We prove the existence of independence paradox in gradient-driven sparsity, which causes error gap in loss change for measuring weight importance.
- We reveal the essence of supermask training is to accumulate weights gradients in gradient-driven sparsity, which partly solves the independence paradox.
- We propose OptG which further optimizes the gradient-driven sparsity using a novel mask optimizer that overcomes the problem of independence paradox.
- Extensive experiments demonstrate the advantage of the proposed OptG over many existing state-of-the-arts in sparsifying modern CNNs.

## 2. Related Work

This section covers the spectrum of studies on sparsifying CNNs that closely related to our work. A more comprehensive overview can be found in the recent survey (Hoefler et al., 2021).

### 2.1. Sparsity Granularity

The granularity of network sparsity varies from coarse grain to fine grain. The former is indicated to removing the entire channels or filters towards a structured subnetwork (He et al., 2017; Lin et al., 2020a; He et al., 2019). Though well suited to a practical speedup on regular hardware devices, significant performance degradation usually occurs at a high sparse rate (Ding et al., 2018; Luo et al., 2017; He et al., 2020; 2018). The latter removes individual neurons at any location of the network to pursue an unstructured

subnetwork (Han et al., 2015; Mocanu et al., 2018). It has been proved to well retain the performance even under an extremely high sparse rate (Kusupati et al., 2020; Gale et al., 2019). Moreover, many recent efforts also show great promise of unstructured sparse networks in practical acceleration (Gale et al., 2020; Elsen et al., 2020). In particular, recent 2:4 sparse pattern has been well supported by Nvidia A100 GPUs to accomplish  $2\times$  speedups.

### 2.2. When to Sparsify

According to the time point the sparsity is applied, we empirically categorize existing works into three groups (Liu et al., 2021a).

**After-training sparsity** was firstly adopted by the optimal brain damage (LeCun et al., 1989). Since then, the followers obey a three-step pipeline, including model pretraining, parameter removing and network fine-tuning (Han et al., 2015; Molchanov et al., 2017; Ding et al., 2019; Lemaire et al., 2019). Unfortunately, in the cases that pre-trained models are missing and hardware resources are limited, the aforementioned approaches become impractical due to the expensive fine-tuning process.

**Before-training sparsity** attempts to conduct network sparsity on randomly initialized networks for efficient model deployment. Trough removing weights using gradient-driven measurement (Lee et al., 2019; Wang et al., 2020) or heuristic design (Tanaka et al., 2020), a sparse subnetwork can be available in a one-shot manner. Nevertheless, the performance gap of this group still exists compared with the after-training sparsity (Frankle et al., 2020).

**During-training sparsity** has been drawing increasing attention for its performance retaining (Mocanu et al., 2018; Mostafa & Wang, 2019; Lin et al., 2020b). In each training iteration, the parameters will be removed or revived according to a predefined criterion. Consequently, the sparse subnetwork can be obtained in a single training process. For instance, RigL (Evci et al., 2020) re-allocates the removed weights according to their dense gradients, while Sparse Momentum (Dettmers & Zettlemoyer, 2019) considers mean momentum magnitude of each layer as a redistribution criterion. Besides, the performance of during-training sparsity can be further enhanced if the desired sparsity is gradually achieved in an incremental manner (Zhu & Gupta, 2017; Liu et al., 2021a;b).

### 2.3. Layer-wise Sparsity Allocation

It has been a wide consensus in the community that layer-wise sparsity allocation, *i.e.*, sparse rate of each layer, is a core in network sparsity (Liu et al., 2019; Gale et al., 2019; Lee et al., 2020). Majorities of existing methods implement layer-wise sparsity using a static or dynamic

design (Evci et al., 2020; Lee et al., 2020). Typically, the global sorting manner also leads to a non-uniform sparsity allocation (Han et al., 2015). Unfortunately, as pointed by (Tanaka et al., 2020), this may result in an extremely imbalanced sparsity budget that parameters in some layers are mostly removed, which further disables the network training. Therefore, recent studies (Kusupati et al., 2020; Savarese et al., 2019) pursue the layer-wise sparsity in a trainable manner, which, however, requires a complex hyper-parameter tuning and often leads to an unstable sparse rate.

#### 2.4. Lottery Ticket Hypothesis and the Supermask

The lottery ticket hypothesis (Frankle & Carbin, 2019) reveals that there exist randomly-initialized sparse networks that can be trained independently to match the performance of the dense model. Following this conjecture, recent empirical studies (Zhou et al., 2019; Ramanujan et al., 2020) have further confirmed the existence of supermask, which simply updates the mask values to obtain sparse subnetworks using the straight-through-estimator (STE) (Bengio et al., 2013) without the necessity of modifying weight values. For instance, (Ramanujan et al., 2020) showed that a randomly initialized Wide ResNet-50 sparsified by a supermask, can match the performance of ResNet-32 trained on ImageNet. (Orseau et al., 2020; Pensia et al., 2020) further proved that the existence of supermask relies on a logarithmic over-parameterization. Despite the progress, an in-depth analysis remains unexplored on why a subnet exists without modifying weight values.

### 3. Method

#### 3.1. Background

**Notations.** Denoting the weights of a convolution neural network as  $\mathbf{w} \in \mathbb{R}^N$  where  $N$  is the weight number, network sparsity can be viewed as multiplying a binary mask  $\mathbf{m} \in \{0, 1\}^N$  on  $\mathbf{w}$  as  $(\mathbf{w} \odot \mathbf{m})$  where  $\odot$  represents the element-wise product. Consequently, the state of the  $i$ -th mask  $\mathbf{m}_i$  indicates whether  $\mathbf{w}_i$  is removed (0) or not (1).

Let  $\mathcal{L}(\cdot)$  and  $\mathcal{D}$  be the training loss and training dataset. Essentially, given a sparse rate  $P$ , network sparsity aims to obtain a sparse  $\mathbf{m}$  subject to  $\frac{\|\mathbf{m}\|_0}{N} \leq 1 - P$ , meanwhile minimizing  $\mathcal{L}(\cdot)$  on  $\mathcal{D}$ . To this end, various scenarios have been proposed to derive  $\mathbf{m}$ . In what follows, we discuss two cases that are mostly related to our method.

**Gradient-driven sparsity.** The studies of network sparsity using weight gradient date back to the last few decades (Le-Cun et al., 1989; Mozer & Smolensky, 1989). The basic idea of these methods is to leverage weight gradients to approximate change in the loss function  $\mathcal{L}(\cdot)$  when removing some

parameters. The overall optimization can be formulated as:

$$\min_{\mathbf{w}} \mathcal{L}(\mathbf{w} \odot \mathbf{m}; \mathcal{D}) \quad s.t. \quad \frac{\|\mathbf{m}\|_0}{N} \leq 1 - P. \quad (1)$$

Then, it is easy to know that the loss change after removing a single weight  $\mathbf{w}_i$  is:

$$\Delta \mathcal{L}(\mathbf{w}_i; \mathcal{D}) = \mathcal{L}(\mathbf{m}_i = 0; \mathcal{D}) - \mathcal{L}(\mathbf{m}_i = 1; \mathcal{D}). \quad (2)$$

It is intuitive that  $\Delta \mathcal{L}(\mathbf{w}_i; \mathcal{D}) < 0$  indicates a loss drop, which means the removal of  $\mathbf{w}_i$  results in better performance. To obtain a sparse  $\mathbf{m}$ , one naive approach is to repeatedly compute the loss change for each weight in  $\mathbf{w}$ , and then set masks of these parameters with larger loss changes to 0s, and 1s otherwise. However, modern CNNs tend to have parameters in millions, making it expensive to perform this one-by-one loss calculation.

Fortunately,  $\Delta \mathcal{L}(\mathbf{w}_i; \mathcal{D})$  can be approximated via the Taylor series expansion. Considering the first-order case (Molchanov et al., 2017),  $\Delta \mathcal{L}(\mathbf{w}_i; \mathcal{D})$  can be reformulated as:

$$\begin{aligned} \Delta \mathcal{L}(\mathbf{w}_i; \mathcal{D}) &= \mathcal{L}(\mathbf{m}_i = 0; \mathcal{D}) - \mathcal{L}(\mathbf{m}_i = 1; \mathcal{D}) \\ &= \mathcal{L}(\mathbf{m}_i = 1; \mathcal{D}) - \frac{\partial \mathcal{L}}{\partial (\mathbf{w}_i \odot \mathbf{m}_i)} (\mathbf{w}_i \odot \mathbf{m}_i) \\ &\quad + R_1(\mathbf{m}_i = 0) - \mathcal{L}(\mathbf{m}_i = 1; \mathcal{D}) \\ &= -\frac{\partial \mathcal{L}}{\partial (\mathbf{w}_i \odot \mathbf{m}_i)} (\mathbf{w}_i \odot \mathbf{m}_i) + R_1(\mathbf{m}_i = 0). \end{aligned} \quad (3)$$

If we ignore the first-order remainder  $R_1(\mathbf{m}_i = 0)$ , then:

$$\Delta \mathcal{L}(\mathbf{w}_i; \mathcal{D}) \approx -\frac{\partial \mathcal{L}}{\partial (\mathbf{w}_i \odot \mathbf{m}_i)} (\mathbf{w}_i \odot \mathbf{m}_i). \quad (4)$$

Eq. (4) can be an efficient alternative to approximating  $\Delta \mathcal{L}(\mathbf{w}_i; \mathcal{D})$ , since for all weights, the term  $\mathbf{w}_i \odot \mathbf{m}_i$  can be available in a single forward propagation and the term  $-\frac{\partial \mathcal{L}}{\partial (\mathbf{w}_i \odot \mathbf{m}_i)}$  can be derived in a single backward propagation. Consequently, the format of Eq. (4) has served as a basic in modern gradient-driven network sparsity (Mozer & Smolensky, 1989). Many recent variants are further excavated based on this format. Taylor-FO (Molchanov et al., 2017) considers  $(\frac{\partial \mathcal{L}}{\partial \mathbf{w}} \odot \mathbf{w})^2$  as a saliency metric to sparsify a pre-trained model, which is similar to the prune-at-initialization SNIP (Lee et al., 2019) that uses  $|\frac{\partial \mathcal{L}}{\partial \mathbf{w}} \odot \mathbf{w}|$  instead. GrasP (Wang et al., 2020) leverages the second-order Taylor series and derives the pruning criterion of  $-\mathbf{H} \frac{\partial \mathcal{L}}{\partial \mathbf{w}} \mathbf{w}$ , where  $\mathbf{H}$  denotes the Hessian matrix. Besides, another variant  $|\frac{\partial \mathcal{L}}{\partial (\mathbf{w}_i \odot \mathbf{m}_i)}|$  is used to indicate if some pruned weights should be revived during sparse training.

Though great effort has been made, these existing works are developed on premise of independence assumption that

weights are irrelevant to each other, which however, is on the contrary in practice as elaborately in Sec. 3.2. As results, their performance remains an open issue.

**Supermask-driven sparsity.** In gradient-driven sparsity, the values of weight vector  $\mathbf{w}$  are updated in the backward propagation and the mask  $\mathbf{m}$  is recomputed using the above criterion in the forward propagation. Instead, many recent developments reveal that a sparse subnet can be found in an untrained network without the necessity of modifying any weight (Zhou et al., 2019). Typically, these methods can be complemented by updating the mask vector  $\mathbf{m}$ . The corresponding learning objective can be formulated as:

$$\min_{\mathbf{m}} \mathcal{L}(\mathbf{w} \odot \mathbf{m}; \mathcal{D}) \quad s.t. \quad \frac{\|\mathbf{m}\|_0}{N} \leq 1 - P. \quad (5)$$

To stress, the objective of Eq. (5) differs from that of Eq. (1) in that its optimized variable is  $\mathbf{m}$  instead of  $\mathbf{w}$  which instead is regarded as a constant vector in Eq. (5). Existing studies (Zhou et al., 2019; Ramanujan et al., 2020) optimize Eq. (5) by first relaxing the discrete  $\mathbf{m} \in \{0, 1\}^N$  to a continuous version of  $\hat{\mathbf{m}} \in \mathbb{R}^N$ . Then, in the forward propagation, a binary function  $h(\cdot)$  is applied to discretize  $\hat{\mathbf{m}} \in \mathbb{R}^N$  as:

$$h(\hat{\mathbf{m}}_i) = \begin{cases} 0, & \text{if } \hat{\mathbf{m}}_i \text{ in the top-}P \text{ smallest of } \hat{\mathbf{m}}, \\ 1, & \text{otherwise.} \end{cases} \quad (6)$$

In the backward propagation, due to the non-differentiable in above equation, the straight-through estimator (STE) (Ben-gio et al., 2013) is used as an alternative to approximate the mask gradient as:

$$\begin{aligned} \frac{\partial \mathcal{L}}{\partial \hat{\mathbf{m}}_i} &= \frac{\partial \mathcal{L}}{\partial (h(\hat{\mathbf{m}}_i) \odot \mathbf{w}_i)} \frac{\partial (h(\hat{\mathbf{m}}_i) \odot \mathbf{w}_i)}{\partial h(\hat{\mathbf{m}}_i)} \frac{h(\hat{\mathbf{m}}_i)}{\hat{\mathbf{m}}_i} \\ &\approx \frac{\partial \mathcal{L}}{\partial (h(\hat{\mathbf{m}}_i) \odot \mathbf{w}_i)} \frac{\partial (h(\hat{\mathbf{m}}_i) \odot \mathbf{w}_i)}{\partial h(\hat{\mathbf{m}}_i)} \\ &= \frac{\partial \mathcal{L}}{\partial (h(\hat{\mathbf{m}}_i) \odot \mathbf{w}_i)} \mathbf{w}_i. \end{aligned} \quad (7)$$

By updating  $\hat{\mathbf{m}}$ , a high-performing sparse subnet can be finally located. Nevertheless, to date, no one has dived into an exploration of why a subnet exists without modifying weight values. In what follows, we give a detailed explanation and show that gradient-driven sparsity and supermask-driven sparsity are the same in essence.

### 3.2. Independence Paradox

The gradient-driven sparsity using Eq. (4) neglects the high-order terms of Taylor series as well as the remainder. Luckily, it has been experimentally proved that the first-order gradient (Lee et al., 2019) shows performance on par with the higher-order ones (Wang et al., 2020). Nevertheless, existing gradient-driven sparsity is built upon the assumption

that weights are irrelevant to each other, which is contrary to the practical implementation (Molchanov et al., 2017; Lee et al., 2019) where a large number of weights are usually removed simultaneously. Considering the case that two weights  $\mathbf{w}_i$  and  $\mathbf{w}_j$  are removed, if independent, the loss change of removing  $\mathbf{w}_i$  using Eq. (3) is:

$$\Delta \mathcal{L}(\mathbf{w}_i; \mathcal{D}) = \mathcal{L}(\mathbf{m}_i = 0, \mathbf{m}_j = 1, \mathbf{w}; \mathcal{D}) - \mathcal{L}(\mathbf{m}_i = 1, \mathbf{m}_j = 1, \mathbf{w}; \mathcal{D}). \quad (8)$$

However, considering that  $\mathbf{w}_j$  has been removed as well, the actual loss change due to the removal of  $\mathbf{w}_i$  should become:

$$\Delta \mathcal{L}(\mathbf{w}_i^*; \mathcal{D}) = \mathcal{L}(\mathbf{m}_i = 0, \mathbf{m}_j = 0, \mathbf{w}^*; \mathcal{D}) - \mathcal{L}(\mathbf{m}_i = 1, \mathbf{m}_j = 0, \mathbf{w}^*; \mathcal{D}), \quad (9)$$

where  $\mathbf{w}^*$  indicates the state of original  $\mathbf{w}$  after the removal of  $\mathbf{w}_j$  and a follow-up fine-tuning on the dataset  $\mathcal{D}$ . It is easy to know that weight-independent Eq. (8) is actually built upon premise of preserving  $\mathbf{w}_j$ . However, the practice removes  $\mathbf{w}_i$  and  $\mathbf{w}_j$  simultaneously, which indicates a loss change of Eq. (9). Thus, there exists an independence paradox in existing studies and the error gap in gradient-driven sparsity is proportional to the total number of removed weights each time.

Note that, some recent advances (Evci et al., 2020; Zhu & Gupta, 2017) advocate incremental pruning that removes a small portion of weights each time. For instance, RigL (Evci et al., 2020) removes a small fraction of weights and activates new ones iteratively, while (Zhu & Gupta, 2017) proposed to gradually increase the number of removed weights until the desired sparse rate is satisfied. Though not explicitly stated, these works indeed accomplish network sparsity by reducing the removed parameters so as to relieve the error gap. Nevertheless, error gap still exists and thus their performance is sub-optimal. An in-depth exploration to overcome this independence paradox remains to be done.

### 3.3. Our Insights on Supermask-driven Sparsity

In this subsection, we show that the success of supermask-driven sparsity is to use the first-order based gradient-driven sparsity in essence. Also, supermask-driven sparsity, to some extent, mitigates the aforementioned independence paradox. Specifically, we denote the mask  $\hat{\mathbf{m}}_i$  at the  $t$ -th training iteration as  $\hat{\mathbf{m}}_i^t$ . Combining the mask gradient in Eq. (7),  $\hat{\mathbf{m}}_i^t$  can be derived via SGD as:

$$\begin{aligned} \hat{\mathbf{m}}_i^t &= \hat{\mathbf{m}}_i^{t-1} - \eta \frac{\partial \mathcal{L}}{\partial \hat{\mathbf{m}}_i^t} \\ &= \hat{\mathbf{m}}_i^{t-1} - \eta \frac{\partial \mathcal{L}}{\partial (h(\hat{\mathbf{m}}_i^t) \odot \mathbf{w}_i)} \mathbf{w}_i, \end{aligned} \quad (10)$$

where  $\eta$  indicates the learning rate. When  $h(\hat{\mathbf{m}}_i^t) = 1$ , we have  $(h(\hat{\mathbf{m}}_i^t) \odot \mathbf{w}_i) = \mathbf{w}_i$ , which leads Eq. (10) to the result



of Eq. (4). When  $h(\hat{\mathbf{m}}_i) = 0$ , which indicates a removal of  $\mathbf{w}_i$ , the computing result of Eq. (10) remains unclear. We show that this can be optimized by adding back the pruned weight  $\mathbf{w}_i$  and the corresponding loss change can be computed as:

$$\begin{aligned}
 \Delta^+ \mathcal{L}(\mathbf{w}_i; \mathcal{D}) &= \mathcal{L}(\mathbf{m}_i = 1; \mathcal{D}) - \mathcal{L}(\mathbf{m}_i = 0; \mathcal{D}) \\
 &= \mathcal{L}(\mathbf{m}_i = 0; \mathcal{D}) - \frac{\partial \mathcal{L}}{\partial (h(\hat{\mathbf{m}}_i) \odot \mathbf{w}_i)} (0 - \mathbf{w}_i) \\
 &\quad + R_1(\mathbf{m}_i = 1) - \mathcal{L}(\mathbf{m}_i = 0; \mathcal{D}) \\
 &= \frac{\partial \mathcal{L}}{\partial (h(\hat{\mathbf{m}}_i) \odot \mathbf{w}_i)} (h(\hat{\mathbf{m}}_i) \odot \mathbf{w}_i) + R_1(\mathbf{m}_i = 1) \\
 &\approx \frac{\partial \mathcal{L}}{\partial (h(\hat{\mathbf{m}}_i) \odot \mathbf{w}_i)} (h(\hat{\mathbf{m}}_i) \odot \mathbf{w}_i) \\
 &= \frac{\partial \mathcal{L}}{\partial (h(\hat{\mathbf{m}}_i) \odot \mathbf{w}_i)} \mathbf{w}_i.
 \end{aligned} \tag{11}$$

This is exactly the pursued mask gradient in Eq. (10). Thus, the updating rule of  $\hat{\mathbf{m}}_i$  can be organized as:

$$\hat{\mathbf{m}}_i^t = \begin{cases} \hat{\mathbf{m}}_i^{t-1} + \eta \Delta \mathcal{L}(\mathbf{w}_i; \mathcal{D}), & \text{if } h(\hat{\mathbf{m}}_i^{t-1}) = 1, \\ \hat{\mathbf{m}}_i^{t-1} - \eta \Delta^+ \mathcal{L}(\mathbf{w}_i; \mathcal{D}), & \text{otherwise.} \end{cases} \tag{12}$$

As defined in Sec. 3.1,  $\Delta \mathcal{L}(\mathbf{w}_i; \mathcal{D})$  is the loss change after removing  $\mathbf{w}_i$  and we expect a small value of  $\Delta \mathcal{L}(\mathbf{w}_i; \mathcal{D})$  if  $\mathbf{w}_i$  is important to the network performance. Similarly, a small  $\Delta^+ \mathcal{L}(\mathbf{w}_i; \mathcal{D})$  also indicates the removed weight is vital to the network and should be revived in the case of supermask-driven sparsity.

Overall, from Eq. (12), we can know that the updating in supermask-driven sparsity is indeed to accumulate gradients of both preserved and removed weights in gradient-driven sparsity. Thus, we can conclude that the manner of supermask-driven sparsity to obtain a sparse mask  $\mathbf{m}$  is indeed similar to that of gradient-driven sparsity. This well explains why supermask-driven sparsity can perform well in existing studies.

Further, we show that the key in supermask training is that it partially solves the independence paradox. Similarly, given that  $\mathbf{w}_i$  and  $\mathbf{w}_j$  are removed at the  $(t-1)$ -th training iteration, we have  $h(\hat{\mathbf{m}}_i^{t-1}) = 1$ . According to Eq. (12), the loss change for adding back  $\mathbf{w}_i$  becomes:

$$\begin{aligned}
 \Delta^+ \mathcal{L}(\mathbf{w}_i; \mathcal{D}) &= \mathcal{L}(\mathbf{m}_i = 1, \mathbf{m}_j = 0, \mathbf{w}; \mathcal{D}) \\
 &\quad - \mathcal{L}(\mathbf{m}_i = 0, \mathbf{m}_j = 0, \mathbf{w}; \mathcal{D}).
 \end{aligned} \tag{13}$$

Obviously, Eq. (13) is closer to the actual loss change of Eq. (9) than independent-based Eq. (8). Thus, the error gap from independence paradox can be well compensated by reviving  $\mathbf{w}_i$  if it is important to the network performance.

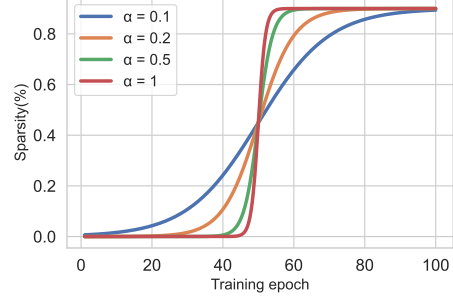


Figure 1. The progression of the overall sparsity with different  $\alpha$  over the course of training by our OptG (90% sparse ResNet-50 on ImageNet).

### 3.4. Optimizing Gradient-driven Sparsity

Herein, we propose to interleave the supermask training into during-training learning to further optimize the gradient-driven sparsity. The learning objective of our method, termed OptG, can be formulated as:

$$\min_{\mathbf{m}, \mathbf{w}} \mathcal{L}(\mathbf{w} \odot \mathbf{m}; \mathcal{D}) \quad \text{s.t.} \quad \frac{\|\mathbf{m}\|_0}{N} \leq 1 - P. \tag{14}$$

The motive of our OptG is to conduct weight optimization and mask training simultaneously. Therefore, when  $\mathbf{w}_j$  is pruned, the remaining weights are further trained on  $\mathcal{D}$  and the update item of  $\hat{\mathbf{m}}_i$  in the  $t$ -th training iteration is:

$$\begin{aligned}
 \Delta \mathcal{L}(\mathbf{w}_i; \mathcal{D}) &= \mathcal{L}(\mathbf{m}_i = 1, \mathbf{m}_j = 0, \mathbf{w}^t; \mathcal{D}) \\
 &\quad - \mathcal{L}(\mathbf{m}_i = 0, \mathbf{m}_j = 0, \mathbf{w}^t; \mathcal{D}),
 \end{aligned} \tag{15}$$

where  $\mathbf{w}^t$  is the trained weights after the  $t$ -th training iteration. Nevertheless, it is clear that  $\mathbf{w}^t$  barely reflects the weight tuning on the whole training set as  $\mathbf{w}^t$  has been trained only for one iteration. Moreover, if the binary function  $h(\cdot)$ , i.e., Eq. (6), is applied during each forward propagation of masks, the network typology may be changed frequently, which can lead to unstable training process.

To solve the above-mentioned problem, we introduce a novel supermask optimizer towards comprehensively solving the independence paradox. In particular, we apply  $h(\cdot)$  to revive and prune weights at the beginning of each training epoch. Then, we continuously accumulate the mask gradient during each training iteration via Eq. (10), but keep the binary mask fixed. Therefore, the preserved weights can be sufficiently retrained on the training set, enabling our mask updating process to finally reach Eq. (9). Note that our OptG sorts the weights in a global manner to automatically decide a layer-wise sparsity budget, thus avoiding the rule-of-thumb design (Evci et al., 2020) or complex hyper-parameter tuning for learning sparsity distributions (He et al., 2018).

**Algorithm 1** Optimizing the gradient-driven sparsity.

---

**Require:** Network weights  $\mathbf{w}$  and masks  $\hat{\mathbf{m}}$ , target sparsity  $P$ , total training epoch  $\tau$ .

- 1:  $\mathbf{w} \leftarrow$  randomly initialization,  $\hat{\mathbf{m}} \leftarrow \mathbf{0}$ ;
- 2: **for**  $k \leftarrow 1, 2, \dots, \tau$  **do**
- 3:   Get current sparse rate via Eq. (16);
- 4:   Get  $\mathbf{m}$  from  $\hat{\mathbf{m}}$  via Eq. (6);
- 5:   **for** each training step  $t$  **do**
- 6:     Forward propagation via  $(\mathbf{w} \odot \mathbf{m})$ ;
- 7:     Compute the gradient of  $\hat{\mathbf{m}}$  via Eq. (7);
- 8:     Update  $\mathbf{w}$ ,  $\hat{\mathbf{m}}$  using SGD optimizer;
- 9:   **end for**
- 10: **end for**

---

We choose to increase the sparse rate from 0 to the target sparsity rate  $P$  on the basis of the sigmoid function as:

$$P_k = \frac{P}{1 + e^{-\alpha(k-0.5\tau)}}, \quad (16)$$

where  $k$  and  $\tau$  represent the current and total training epoch,  $\alpha$  is a hyperparameter that controls the total epoch for achieving sparsity. Fig. 1 shows that the sparsity ascent rate at initialization can be relatively smooth. The intuition behind this gradual sparsity schedule is that the weights require sufficient training as reviving a random-initialized weight is usually meaningless from the perspective of Eq. (11). Alternatively, we propose a novel learning rate schedule for the mask training with respect to this sparsity schedule. When the sparse rate of the network is low, the learning rate of masks is also small as the calculation of gradient score will be seriously interfered by the independence paradox. Moreover, when the sparse rate reaches  $P$ , the learning rate of masks can follow weights to sufficiently optimize the gradient-driven criteria while guarantee training convergence. Overall, our optimizer assign the mask learning rate at epoch  $k$  as:

$$\eta_{\hat{\mathbf{m}},k} = \frac{\eta_{\mathbf{w},k}}{1 + e^{-\alpha(k-0.5\tau)}}, \quad (17)$$

where  $\eta_{\mathbf{w},k}$  is the learning rate of weights at the  $k$ -th epoch. We summarize the workflow of the supermask optimizer in Alg. 1.

## 4. Experiments

### 4.1. Settings

We conduct extensive experiments to evaluate the efficacy of our OptG in sparsifying VGGNet-19 (Simonyan & Zisserman, 2015), ResNet-50 (He et al., 2016) on small scale CIFAR-10/100 (Krizhevsky et al., 2009) datasets and ResNet-50 (He et al., 2016), MobileNet-V1 (Howard et al., 2017) on large scale ImageNet (Deng et al., 2009) dataset.

Besides, we compare our OptG with several the state-of-the-arts including SNIP (Lee et al., 2019), GraSP (Wang et al., 2020), Deep-R (Bellec et al., 2018) SynFlow (Tanaka et al., 2020), SET (Mocanu et al., 2018), GMP (Gale et al., 2019), DNW (Wortsman et al., 2019), DSR (Mostafa & Wang, 2019), SNFS (Dettmers & Zettlemoyer, 2019), RigL (Evci et al., 2020), STR (Kusupati et al., 2020) and GraNet (Liu et al., 2021a).

We implement OptG with PyTorch (Paszke et al., 2019). Particularly, we set  $\alpha = 0.5$  in all experiments and leverage the SGD optimizer to update the weights and their masks with a gradually-increasing sparsity rate Eq. (16). On CIFAR-10 and CIFAR-100, we train the networks for 160 epochs with a weight decay of  $1 \times 10^{-3}$ . On ImageNet, the weight decay is set to  $5 \times 10^{-4}$  for ResNet-50 and  $4 \times 10^{-5}$  for MobileNet-V1. We train ResNet-50 for 100 epochs and MobileNet-V1 for 180 epochs, respectively. Besides, the initial learning rate is set to 0.1, which is then decayed by the cosine annealing scheduler during training. All experiments are run with NVIDIA Tesla V100 GPUs.

### 4.2. CIFAR-10/100

**VGGNet-19.** Tab. 1 shows the performance of different methods for sparsifying the classic VGGNet with 19 layers. Compared with the competitors, our OptG yields better accuracy under the same sparse rate both on CIFAR-10

Table 1. Top-1 accuracy (%) for sparsifying VGGNet-19 and ResNet-50 on CIFAR-10/100.

Dataset	CIFAR-10		CIFAR-100	
Sparse Rate	90%	95%	90%	95%
VGGNet-19	93.85	-	73.43	-
Deep-R	90.81	89.59	66.83	63.46
SET	92.46	91.73	72.36	69.81
SNIP	93.63	93.43	72.84	71.83
GraSP	93.30	93.04	92.19	71.95
SynFlow	93.35	93.45	92.24	71.77
STR	93.73	93.27	71.93	71.14
RigL	93.47	93.35	71.82	71.53
GMP	93.59	93.58	73.10	72.30
GraNet	93.80	93.72	73.74	73.10
OptG	<b>93.84</b>	<b>93.72</b>	<b>73.80</b>	<b>73.24</b>
ResNet-50	94.75	-	78.23	-
SNIP	92.65	90.86	73.14	69.25
GraSP	92.47	91.32	73.28	70.29
SynFlow	92.49	91.22	73.37	70.37
STR	92.59	91.35	73.75	70.45
RigL	94.45	93.86	76.50	76.03
GMP	94.34	94.52	76.91	76.42
GraNet	94.49	94.44	77.29	76.71
OptG	<b>94.55</b>	<b>94.56</b>	<b>77.41</b>	<b>77.02</b>

## Optimizing Gradient-driven Criteria in Network Sparsity: Gradient is All You Need

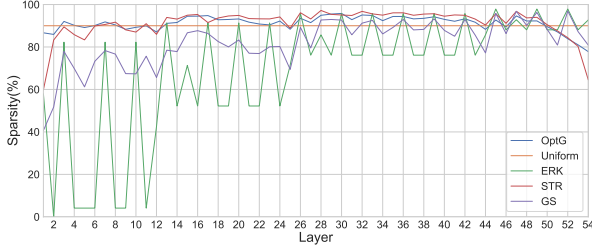


Figure 2. Layer-wise sparsity budget of ResNet-50 on ImageNet at 90% sparse rate.

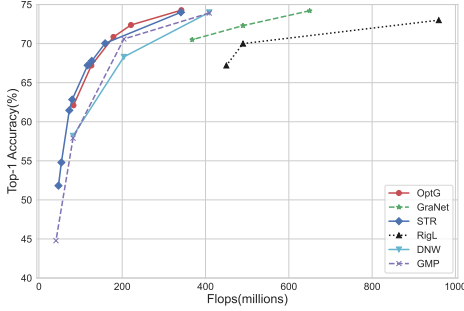


Figure 3. Top-1 accuracy v.s. FLOPs of ResNet-50 on ImageNet.

and CIFAR-100 datasets. For instance, compared with SNIP (Lee et al., 2019) that suffers serious performance degradation of 4.26% when pruning 95% parameters on CIFAR-10 (89.59% for SNIP and 93.85% for the baseline), the proposed OptG only lose negligible accuracy of 0.01% (93.84% for OptG), despite they are both built on gradient information. On CIFAR-100, our OptG provides significantly better accuracy against other gradient-driven approaches including GrasP (Wang et al., 2020) and RigL (Evci et al., 2020), which demonstrates the superiority of optimizing the gradient-driven criteria in network sparsity.

**ResNet-50.** It can also be referred from Tab. 1 that our OptG outperforms the state-of-the-art on both CIFAR-10 and CIFAR-100 datasets. In term of 90% sparse rate on CIFAR-10, OptG improve the performance of other during-training methods including GMP (Tanaka et al., 2020) and STR (Kusupati et al., 2020) by 0.25% and 0.11% (93.84%, 92.49%, 92.59% for OptG, GMP, STR). On CIFAR-100, our method again outperforms the most recent GraNet by 0.12% and 0.31% at 90% and 95% sparsity, respectively. Overall, OptG demonstrates its great capability over other methods to accelerate classic CNNs on small scale datasets.

### 4.3. ImageNet

**ResNet-50.** The comparison of compressing ResNet-50 (He et al., 2016) between the proposed OptG and its counterparts is presented in Tab. 2. As can be seen, our OptG well

Table 2. Performance comparison of ResNet-50 on ImageNet.

Method	Sparsity	Params	FLOPs	Top-1 Acc.
ResNet-50	0.00	25.6M	4.09G	77.01
SNIP	90.00	2.56M	409M	67.20
SET	90.00	2.56M	409M	69.60
GMP	90.00	2.56M	409M	73.91
DNW	90.00	2.56M	409M	74.00
DSR	90.00	2.56M	1.23G	71.60
SNFS	90.00	2.56M	960M	72.90
RigL	90.00	2.56M	960M	73.00
STR	90.55	2.41M	341M	74.01
GraNet	90.00	2.56M	650M	74.20
OptG	90.00	2.56M	342M	<b>74.28</b>
GMP	95.00	1.28M	204M	70.59
DNW	95.00	1.28M	204M	68.30
RigL	95.00	1.28M	490M	70.00
STR	95.03	1.27M	159M	70.40
GraNet	95.00	1.28M	490M	72.30
OptG	95.00	1.28M	221M	<b>72.38</b>
RigL	96.50	0.90M	450M	67.20
STR	96.11	0.99M	127M	67.78
GraNet	96.50	0.90M	368M	70.50
OptG	96.50	0.90M	179M	<b>70.85</b>
GMP	98.00	0.51M	82M	57.90
DNW	98.00	0.51M	82M	58.20
STR	97.78	0.57M	80M	62.84
STR	98.05	0.50M	73M	61.46
OptG	98.00	0.51M	126M	<b>67.20</b>
GMP	99.00	0.26M	41M	44.78
STR	98.98	0.26M	47M	51.82
STR	98.79	0.31M	54M	54.79
OptG	99.00	0.26M	83M	<b>62.10</b>

surpasses its competitors across different sparse rates. For example, in comparison with the gradient-driven approach RigL at a sparse rate of 90%, OptG greatly reduces the FLOPs to 342M with a remarkable accuracy of 74.28%, while RigL only reaches 73.00% with much higher FLOPs of 960M. When the sparse rate reaches 98.00%, all existing studies suffer severe performance degradation. In contrast, OptG presents an amazing result of 67.20% top-1 accuracy, which well surpasses the recent advances of STR by 4.36% and DNW by 9.00%. Furthermore, at an extreme sparse rate of around 99.00%, the proposed OptG still retains a high accuracy of 62.10%, which surpasses the second best STR by a large margin. These comparison results well demonstrate the efficacy of our OptG in compressing the large-scale ResNet.

Besides, it is worth mentioning that our OptG well outperforms STR by large margins across various sparse rates,

### Optimizing Gradient-driven Criteria in Network Sparsity: Gradient is All You Need

Table 3. Performance comparison of MobileNet-V1 on ImageNet.

Method	Sparsity	Params	FLOPs	Top-1 Acc.
MobileNet-V1	0.00	4.12M	569M	71.95
GMP	74.11	1.09M	163M	67.70
STR	75.28	1.04M	101M	68.35
STR	79.07	0.88M	81M	66.52
OptG	80.00	0.82M	124M	<b>70.27</b>
GMP	89.03	0.46M	82M	61.80
STR	85.80	0.60M	55M	64.83
STR	89.01	0.46M	42M	62.10
STR	89.62	0.44M	40M	61.51
OptG	90.00	0.41M	80M	<b>66.80</b>

despite that STR has to conduct complex hyper-parameter tuning to obtain the overall sparsity, while OptG is much more flexible via a simple one-shot global sorting. To dive into a deeper analysis, given an overall sparse rate of 90%, we display the layer-wise sparsity budget in Fig. 2. Compared with other methods, on one hand, our OptG automatically assigns non-uniform sparsity budget across layers; on the other hand, it can allocate more budgets for the shallow layers, which contain more FLOPs than the deeper layers. This well explains why the FLOPs reduction of our OptG can be better than others when similar parameters are removed. As shown in Fig. 3, OptG again leads a frontier curve over other approaches for the accuracy performance under a similar FLOPs reduction. Although STR shows comparable accuracy, its performance is built upon preserving more parameters as displayed in Tab. 2. For example, our OptG obtains top-1 accuracy of 67.20% with 126M FLOPs and 0.51M parameters. In contrast, STR obtains a slightly better top-1 accuracy of 67.78% at the cost of more FLOPs of 127M and parameters of 0.99M.

**MobileNet-V1.** MobileNet-V1 (Howard et al., 2017) is a lightweight network with depth-wise convolution. Thus, compared with ResNet-50, it is more different to sparsify MobileNet-V1 without performance compromise. Nevertheless, results on Tab. 3 shows that our OptG still offers reliable performance on such a challenging task. Specifically, OptG achieves a top-1 accuracy of 70.27% at a sparse rate of 89.00%, which is 3.75% higher than that of STR that suffers more parameter burden as well. Similar observation can be found when the sparse rate is around 90.00%. Our OptG reduces the parameters to 0.41M and FLOPs to 80M, meanwhile it still preserve an accuracy of 66.80%. As for STR at a sparse rate of only 80.00%, it obtains a lower accuracy of 66.52%. Thus, OptG well demonstrates its ability to sparsify lightweight networks.

#### 4.4. Ablation Studies

**The gradual sparsity schedule.** Tab. 4 shows the accuracy of different sparsity techniques under the same gradual

Table 4. Performance of different methods for sparsifying ResNet-50 on ImageNet under the same gradual sparsity schedule.

Method	Sparsity	Params	FLOPs	Top-1 Acc.
SET	90.00	5.12M	409M	67.19
RigL	90.00	5.12M	960M	72.02
GMP	90.00	5.12M	409M	73.80
OptG	90.00	5.12M	342M	<b>74.28</b>

Table 5. Performance of our OptG for sparsifying ResNet-50 on ImageNet with different layer-wise sparsity budget.

Method	Sparsity	Params	FLOPs	Top-1 Acc.
Uniform	90.00	5.12M	409M	74.12
GS	90.00	5.12M	697M	73.89
ERK	90.00	5.12M	960M	<b>74.39</b>
OptG	90.00	5.12M	342M	74.28

sparsity schedule as defined in Eq. (16). Therefore, the difference among OptG and other methods falls in how to revive and prune weights in the during-training sparsity. As can be observed, OptG still take the lead over all methods, thus well demonstrates our point of optimizing the gradient-driven criteria.

It is worth mentioning that applying our schedule to other methods even leads to worth performance comparing with their origin schedule. This is reasonable for that other methods generally revive weights to 0s, which, if carried out in the latter training process, can not ensure a sufficient training. Therefore, different motivations lead to a unique sparse schedule for our OptG.

**Layer-wise sparsity budgets.** We further investigate the effect of layer-wise sparsity budgets by only sorting the weights inter-layer while keeping the layer-wise sparsity fixed with respect to different pre-defined budgets including Uniform, GS (Han et al., 2015), ERK (Evci et al., 2020). As can be seen, using the global magnitude pruning (GS) as well as uniform budget both lead to accuracy drop. The ERK budget can achieve better performance with our global-sorting mechanism, nevertheless, the FLOPs of ERK is much higher than the layer-wise budget automatically decided by OptG. Therefore, the efficacy of sparsity budget chosen for OptG is also well identified.

## 5. Conclusion

In this paper, we have proposed to optimize the gradient-driven criteria in network sparsity, termed OptG. In particular, we first point out the independence paradox in previous approaches and show an effective trail to solve this paradox based on revealing the empirical success of supermask training. Following this trail, we further propose to solve the independence paradox by interleaving the supermask training process into during-training sparsity with a novel su-



permask optimizer. Extensive experiments on various tasks demonstrate that our OptG can automatically obtain layer-wise sparsity burden, while achieving state-of-the-art performance at all sparsity regimes. Our work re-emphasizes the great potential of gradient-driven pruning and we expect future advances for the gradient-driven criteria optimizer.

## 6. Acknowledge

This work is supported by the National Science Fund for Distinguished Young Scholars (No.62025603), the National Natural Science Foundation of China (No.U1705262, No.62072386, No.62072387, No.62072389, No.62002305, No.61772443, No.61802324 and No.61702136) and Guangdong Basic and Applied Basic Research Foundation (No.2019B1515120049).

## References

- Bellec, G., Kappel, D., Maass, W., and Legenstein, R. Deep rewiring: Training very sparse deep networks. In *International Conference on Learning Representations (ICLR)*, 2018.
- Bengio, Y., Léonard, N., and Courville, A. Estimating or propagating gradients through stochastic neurons for conditional computation. *arXiv preprint arXiv:1308.3432*, 2013.
- Deng, J., Dong, W., Socher, R., Li, L.-J., Li, K., and Fei-Fei, L. Imagenet: A large-scale hierarchical image database. In *IEEE Conference on Computer Vision and Pattern Recognition (CVPR)*, pp. 248–255, 2009.
- Dettmers, T. and Zettlemoyer, L. Sparse networks from scratch: Faster training without losing performance. In *Advances in Neural Information Processing Systems (NeurIPS)*, 2019.
- Ding, X., Ding, G., Han, J., and Tang, S. Auto-balanced filter pruning for efficient convolutional neural networks. In *Proceedings of the AAAI Conference on Artificial Intelligence (AAAI)*, volume 32, 2018.
- Ding, X., Ding, G., Guo, Y., and Han, J. Centripetal sgd for pruning very deep convolutional networks with complicated structure. In *IEEE Conference on Computer Vision and Pattern Recognition (CVPR)*, pp. 4943–4953, 2019.
- Elsen, E., Dukhan, M., Gale, T., and Simonyan, K. Fast sparse convnets. In *IEEE Conference on Computer Vision and Pattern Recognition (CVPR)*, pp. 14629–14638, 2020.
- Evci, U., Gale, T., Menick, J., Castro, P. S., and Elsen, E. Rigging the lottery: Making all tickets winners. In *International Conference on Machine Learning (ICML)*, pp. 2943–2952, 2020.
- Frankle, J. and Carbin, M. The lottery ticket hypothesis: Finding sparse, trainable neural networks. In *International Conference on Learning Representations (ICLR)*, 2019.
- Frankle, J., Dziugaite, G. K., Roy, D. M., and Carbin, M. Pruning neural networks at initialization: Why are we missing the mark? *arXiv preprint arXiv:2009.08576*, 2020.
- Gale, T., Elsen, E., and Hooker, S. The state of sparsity in deep neural networks. *arXiv preprint arXiv:1902.09574*, 2019.
- Gale, T., Zaharia, M., Young, C., and Elsen, E. Sparse gpu kernels for deep learning. In *International Conference for High Performance Computing, Networking, Storage and Analysis*, pp. 1–14, 2020.
- Han, S., Pool, J., Tran, J., and Dally, W. Learning both weights and connections for efficient neural network. In *Advances in Neural Information Processing Systems (NeurIPS)*, pp. 1135–1143, 2015.
- He, K., Zhang, X., Ren, S., and Sun, J. Deep residual learning for image recognition. In *IEEE Conference on Computer Vision and Pattern Recognition (CVPR)*, pp. 770–778, 2016.
- He, Y., Zhang, X., and Sun, J. Channel pruning for accelerating very deep neural networks. In *IEEE Conference on Computer Vision and Pattern Recognition (CVPR)*, pp. 1389–1397, 2017.
- He, Y., Kang, G., Dong, X., Fu, Y., and Yang, Y. Soft filter pruning for accelerating deep convolutional neural networks. In *International Joint Conference on Artificial Intelligence (IJCAI)*, pp. 2234–2240, 2018.
- He, Y., Liu, P., Wang, Z., Hu, Z., and Yang, Y. Filter pruning via geometric median for deep convolutional neural networks acceleration. In *IEEE Conference on Computer Vision and Pattern Recognition (CVPR)*, pp. 4340–4349, 2019.
- He, Y., Ding, Y., Liu, P., Zhu, L., Zhang, H., and Yang, Y. Learning filter pruning criteria for deep convolutional neural networks acceleration. In *IEEE Conference on Computer Vision and Pattern Recognition (CVPR)*, pp. 2009–2018, 2020.
- Hoeffler, T., Alistarh, D., Ben-Nun, T., Dryden, N., and Peste, A. Sparsity in deep learning: Pruning and growth for efficient inference and training in neural networks. *Journal of Machine Learning Research*, 22:1–124, 2021.

- Howard, A. G., Zhu, M., Chen, B., Kalenichenko, D., Wang, W., Weyand, T., Andreetto, M., and Adam, H. Mobilenets: Efficient convolutional neural networks for mobile vision applications. *arXiv preprint arXiv:1704.04861*, 2017.
- Krizhevsky, A., Hinton, G., et al. Learning multiple layers of features from tiny images. 2009.
- Kusupati, A., Ramanujan, V., Somani, R., Wortsman, M., Jain, P., Kakade, S., and Farhadi, A. Soft threshold weight reparameterization for learnable sparsity. In *International Conference on Machine Learning (ICML)*, pp. 5544–5555, 2020.
- LeCun, Y., Denker, J., and Solla, S. Optimal brain damage. In *Advances in Neural Information Processing Systems (NeurIPS)*, pp. 598–605, 1989.
- Lee, J., Park, S., Mo, S., Ahn, S., and Shin, J. Layer-adaptive sparsity for the magnitude-based pruning. In *International Conference on Learning Representations (ICLR)*, 2020.
- Lee, N., Ajanthan, T., and Torr, P. Snip: Single-shot network pruning based on connection sensitivity. In *International Conference on Learning Representations (ICLR)*, 2019.
- Lemaire, C., Achkar, A., and Jodoin, P.-M. Structured pruning of neural networks with budget-aware regularization. In *IEEE Conference on Computer Vision and Pattern Recognition (CVPR)*, pp. 9108–9116, 2019.
- Lin, M., Ji, R., Wang, Y., Zhang, Y., Zhang, B., Tian, Y., and Shao, L. Hrank: Filter pruning using high-rank feature map. In *IEEE Conference on Computer Vision and Pattern Recognition (CVPR)*, pp. 1529–1538, 2020a.
- Lin, T., Stich, S. U., Barba, L., Dmitriev, D., and Jaggi, M. Dynamic model pruning with feedback. In *International Conference on Learning Representations (ICLR)*, 2020b.
- Liu, S., Chen, T., Chen, X., Atashgahi, Z., Yin, L., Kou, H., Shen, L., Pechenizkiy, M., Wang, Z., and Mocanu, D. C. Sparse training via boosting pruning plasticity with neuroregeneration. In *Advances in Neural Information Processing Systems (NeurIPS)*, 2021a.
- Liu, S., Yin, L., Mocanu, D. C., and Pechenizkiy, M. Do we actually need dense over-parameterization? in-time over-parameterization in sparse training. In *International Conference on Machine Learning (ICML)*, 2021b.
- Liu, Z., Sun, M., Zhou, T., Huang, G., and Darrell, T. Re-thinking the value of network pruning. In *International Conference on Learning Representations (ICLR)*, 2019.
- Luo, J.-H., Wu, J., and Lin, W. Thinet: A filter level pruning method for deep neural network compression. In *IEEE International Conference on Computer Vision (ICCV)*, pp. 5058–5066, 2017.
- Mocanu, D. C., Mocanu, E., Stone, P., Nguyen, P. H., Gibescu, M., and Liotta, A. Scalable training of artificial neural networks with adaptive sparse connectivity inspired by network science. *Nature Communications*, 9: 1–12, 2018.
- Molchanov, P., Tyree, S., Karras, T., Aila, T., and Kautz, J. Pruning convolutional neural networks for resource efficient inference. In *International Conference on Learning Representations (ICLR)*, 2017.
- Mostafa, H. and Wang, X. Parameter efficient training of deep convolutional neural networks by dynamic sparse reparameterization. In *International Conference on Machine Learning (ICML)*, pp. 4646–4655, 2019.
- Mozer, M. C. and Smolensky, P. Skeletonization: A technique for trimming the fat from a network via relevance assessment. In *Advances in Neural Information Processing Systems (NeurIPS)*, pp. 107–115, 1989.
- Orseau, L., Hutter, M., and Rivasplata, O. Logarithmic pruning is all you need. In *Advances in Neural Information Processing Systems (NeurIPS)*, pp. 2925–2934, 2020.
- Paszke, A., Gross, S., Massa, F., Lerer, A., Bradbury, J., Chanan, G., Killeen, T., Lin, Z., Gimelshein, N., Antiga, L., et al. Pytorch: An imperative style, high-performance deep learning library. In *Advances in Neural Information Processing Systems (NeurIPS)*, pp. 8026–8037, 2019.
- Pensia, A., Rajput, S., Nagle, A., Vishwakarma, H., and Papailiopoulos, D. Optimal lottery tickets via subset-sum: Logarithmic over-parameterization is sufficient. In *Advances in Neural Information Processing Systems (NeurIPS)*, pp. 2599–2610, 2020.
- Ramanujan, V., Wortsman, M., Kembhavi, A., Farhadi, A., and Rastegari, M. What’s hidden in a randomly weighted neural network? In *IEEE Conference on Computer Vision and Pattern Recognition (CVPR)*, pp. 11893–11902, 2020.
- Savarese, P., Silva, H., and Maire, M. Winning the lottery with continuous sparsification. *arXiv preprint arXiv:1912.04427*, 2019.
- Simonyan, K. and Zisserman, A. Very deep convolutional networks for large-scale image recognition. In *International Conference on Learning Representations (ICLR)*, 2015.
- Tanaka, H., Kunin, D., Yamins, D. L., and Ganguli, S. Pruning neural networks without any data by iteratively conserving synaptic flow. In *Advances in Neural Information Processing Systems (NeurIPS)*, 2020.

Wang, C., Zhang, G., and Grosse, R. Picking winning tickets before training by preserving gradient flow. In *International Conference on Learning Representations (ICLR)*, 2020.

Wortsman, M., Farhadi, A., and Rastegari, M. Discovering neural wirings. In *Advances in Neural Information Processing Systems (NeurIPS)*, pp. 2680–2690, 2019.

Zhou, H., Lan, J., Liu, R., and Yosinski, J. Deconstructing lottery tickets: zeros, signs, and the supermask. In *Advances in Neural Information Processing Systems (NeurIPS)*, pp. 3597–3607, 2019.

Zhu, M. and Gupta, S. To prune, or not to prune: exploring the efficacy of pruning for model compression. In *International Conference on Learning Representations Workshop (ICLRW)*, 2017.